P 2.22 **ENTRAINMENT, MIXING, AND MICROPHYSICS IN RICO CUMULUS**

H. Gerber
Gerber Scientific Inc., Reston, VA, U.S.A.

1. INTRODUCTION

We have known for a long time (Warner, 1955) that small cumulus (Cu) clouds are rapidly diluted as they grow vertically by entraining external air. We have also had a reasonable conceptional idea of how the entrainment proceeds. In this regard a long-lived view has been the "bubble and wake" concept (Scorer and Ludlum, 1953; Blyth et al, 1988) where the top of an ideal cumulus cloud consists of a buoyant bubble which erodes on its front surface as it moves upward, entrains air along its sides, and trails a wake of turbulent and cloudy air. However, our quantitative knowledge of the entrainment process and its effect on cloud microphysics still needs improvement. For example, we don't know how the entrainment and subsequent mixing affect the droplet spectra. Modeling has not resolved this issue as illustrated by Jensen and Baker (1989) and more recently Lasher-Trapp et al (2005). In that work the oft described "homogenous" and "inhomogeneous" mixing mechanisms in Cu cause large but different changes in the spectra and thus can affect coalescence and Cu evolution, but it was not possible to identify which mechanism prevailed. Another poorly known aspect is the scale of the entrained parcels which would affect their lifetime within the Cu and evolution of the spectra.

RICO (Rain in Cumulus over the Ocean) presented an opportunity to further investigate the processes associated with entrainment in small Cu. This comprehensive field study took place in the vicinity of Antigua in the Carribean in Dec. 2004 and Jan. 2005. The work described here deals primarily with the high-resolution PVM-100A measurements made during passes of the NCAR C-130 research aircraft through numerous small trade-wind Cu. This probe measured simultaneously with an incloud resolution of about 10 cm LWC (liquid water content) and PSA (particle surface area) the ratio of which is the Re (effective radius). This resolution is not ideal because it is still about 2 orders of magnitude larger than the Kolmogorov scale where molecular diffusion affects droplet size. Still this resolution is much better than that attainable with droplet spectrometers used on the aircraft, given their much larger statistical sampling errors which for the relatively small droplet concentrations found in the RICO Cu are unwieldy. The following describes how the high-speed PVM-100A data was analyzed for one RICO flight (RF12), and presents some new findings related to entrainment, mixing, and microphysics in trade-wind Cu.

Corresponding author address: Hermann E. Gerber, Gerber Scientific Inc., Reston, VA 20190, email: hgerber6@comcast.net

2. CONDITIONAL SAMPLING

Figure 1 shows all the 1-Hz LWC (~100-m resolution) and some of the 1000 Hz LWC (~10-cm resolution) data collected while the C-130 flew through a total of about 200 Cu predominantly at 5 different levels separated by about 200 m. Also shown is the LWC for precipitation-sized drops measured by the 2DC probe. This figure shows that the rapid reduction of measured LWC with height above cloud base from the calculated adiabatic LWC value reflects the presence of significant entrainment, and shows that adiabatic parcels larger than ~10 cm only exist up to several hundred m above cloud base.

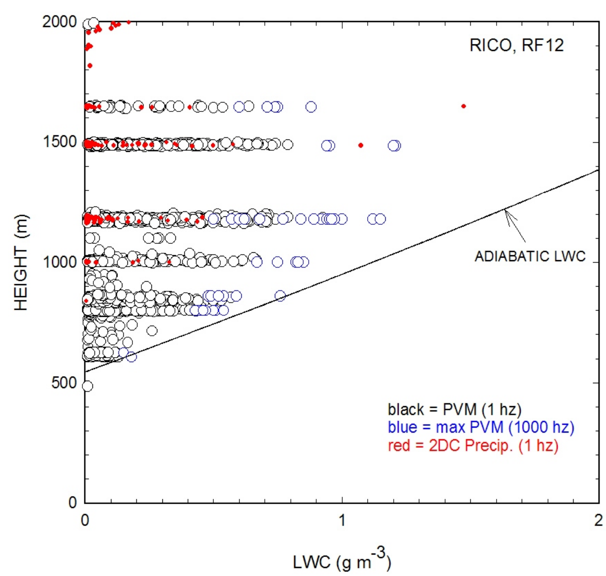

Figure 1 - 100-m resolution (1Hz), maximum 10-cm resolution (1000 Hz),and 2DC LWC for all ~ 200 Cu aircraft passes for flight RF12.

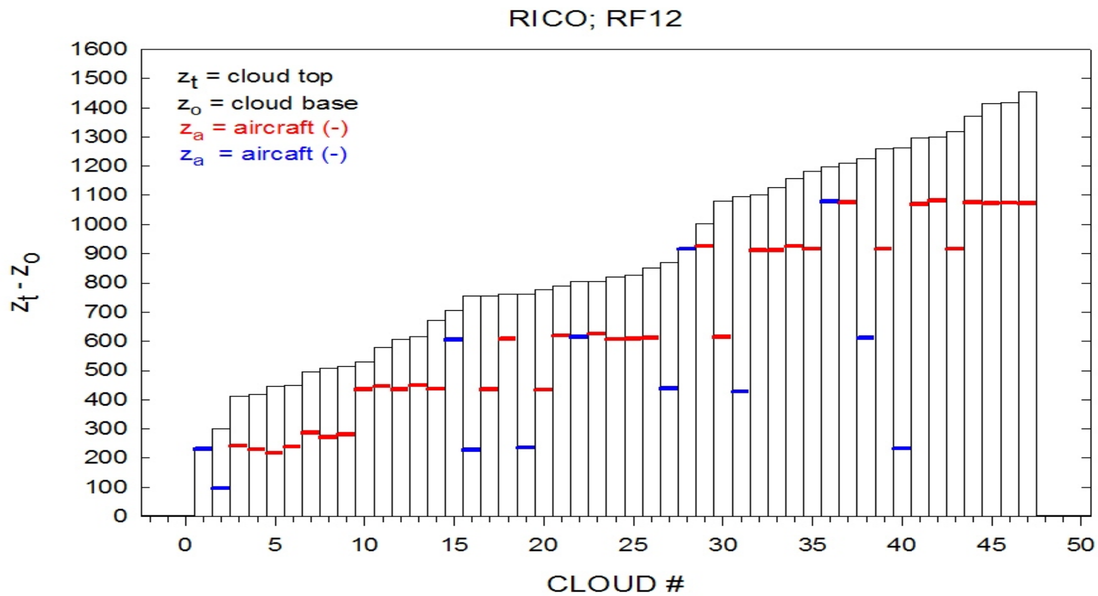

Figure 2 - Histogram of cumulus clouds (red) on flight RF12 chosen by conditional sampling according to the certain conditions (see text); and cumuli (blue) meeting only partial conditions.

Table 1 - General characteristics of the conditionally-sampled 35 Cu on flight RF12, with average values of 7 Cu at each level $z_a - z_o$ flown by the aircraft above cloud base. z_a is the aircraft level z_t is the cloud top height, z_o is cloud base (LCL estimated at 570 m), W is cloud width, LWC is liquid water content, r_v is mean volume radius, LWCa is the expected adiabatic liquid water content, r_{va} is the expected adiabatic mean volume radius, N is the droplet concentration, w is the vertical velocity, w_m is the maximum vertical velocity, is the fractional entrainment rate (total q calculation), and is the TKE dissipation rate incloud.

$z_a - z_o$ (m)	z_t (m)	$z_t - z_a$ (m)	W (m)	LWC (gm^{-3})	r_v (um)	LWCa (gm^{-3})	r_{va} (um)	N (No/cc)	w (ms^{-1})	w_m (ms^{-1})	(m^{-1})	(cm^2/s^3)
252	1009	187	544	.269	9.19	.605	11.4	95	1.18	2.98	.00229	14.0
439	1205	196	484	.387	10.60	1.00	13.5	97	1.25	4.99	.00126	41.3
615	1398	213	453	.485	10.20	1.42	15.2	121	1.92	6.11	.00073	63.2
918	1722	234	612	.510	10.65	2.11	17.3	116	1.90	7.08	.00091	74.6
1074	1920	276	631	.326	11.87	2.46	18.2	54	-.283	3.11	.00612	29.0

A forward-looking digital video was a new feature on the C-130 for the RICO study, and it provided the opportunity to view all the ~200 Cu on flight RF12 and to quantify Cu geometrical features. Viewing these Cu leads to the impression that they reflect a remarkable complexity, with the ideal "bubble and wake" geometry hardly ever observed. Some Cu are vigorous, others are not, others are dissipating and broken, and others form complex clusters. For these reasons it was decided not to analyze all ~ 200 Cu, but to follow in the footsteps of Raga et al (1990) and analyze only those that met a similar conditional sampling criterion. In their study of Hawaiian rain-band Cu they chose several Cu with vigorous updrafts. Here we do the same with some additional conditions: 1) vertical velocity is positive in at least 80% of the Cu [for the bottom 4 levels], 2) the top of the Cu is visible in the video so that the distance between cloud penetration and cloud top can be calculated, 3) the Cu is traversed near cloud top, and 4) Cu consisting of individual turrets are chosen. These rules provided a choice of 47 Cu shown in Fig. 2, with a final choice (heavy red bars) of 7 Cu for each of the 5 levels flown by the C-130. The Cu not chosen in Fig. 2 represented skimming aircraft passes at cloud top, clouds which were fragmented, and deeper cloud passes. The rationales for choosing the RF12 active Cu turrets in this fashion are that these turrets are thought to contain the greatest amount of LWC and thus would lead to the highest probability for coalescence and precipitation initiation, and that the average behavior of the Cu at the 5 levels would permit us to estimate from observation the evolution of entrainment effects and other Cu properties as these Cu grew vertically. Table 1 list some general characteristics of the conditionally sampled Cu at the 5 aircraft levels.

3. HOMOGENEOUS vs INHOMOGENEOUS MIXING

The relationship between LWC and Re measured by the PVM-100A can be written as LWC = 4 ${}_t r_v^3$ ~ 4 ${}_t Re^3$, where ${}_t$ is the total droplet number concentration, and r_v is the mean volume radius. Figure 3 shows a plot of these parameters using the high-rate data for one Cu pass (cloud #21) at ~600-m above cloud base.

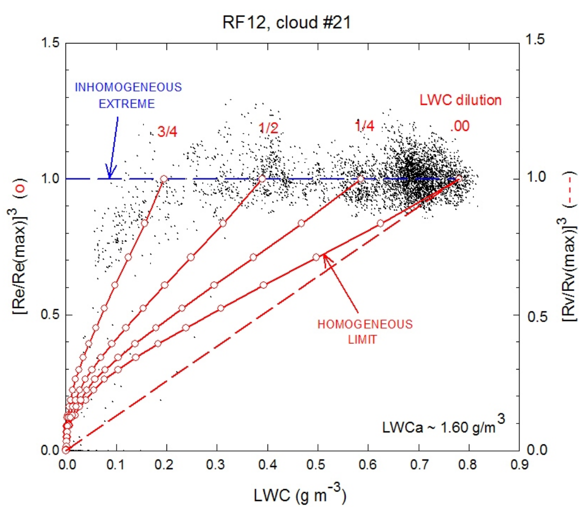

Fig.3 - Normalized effective radius (Re) to maximum Re in Cu pass for cloud #21 as a function of high data-rate LWC.

Here both Re^3 and r_v^3 are normalized by their maximum values found in this Cu. The blue dashed line represents extreme inhomogeneous mixing following entrainment where LWC is decreased without changing the relative shape of the droplet spectrum. The red lines represent homogeneous mixing where reductions in LWC depend on changes in droplet sizes caused by evaporation or growth. The red lines were established using measured FSSP droplet spectra in the Cu, where the changes in drop sizes drops were calculated using the droplet growth equation under the condition that the environment was substantially sub-saturated (at lesser sub-saturations the red lines would not converge at the origin of this plot). The dashed red line represents changes in r_v^3, and the solid red lines changes in Re^3. These changes depend on the initial dilution of the Cu by the cloud-free entrained air which is given by the LWC dilution fraction in red numbers. The homogenous limit is represented by the two bottom red lines and represents changes where no initial dilution is involved. The data points in Fig. 3 suggest that the mixing in this Cu is primarily extreme inhomogeneous given that the data points fall mostly along the horizontal blue line, with only some smaller values of Re^3 at small values of LWC.

A second way of plotting the PVM-100A data for the same Cu is shown in Fig. 4 where the normalized Re^3 is compared to the normalized ${}_t$ calculated from the measured values of LWC and Re. This approach has been used previously (Gerber et al., 2001) for some SCMS (Small Cumulus Microphysics Study), and more recently by Burnet and Brenguier (2006) and Schlueter (2006).

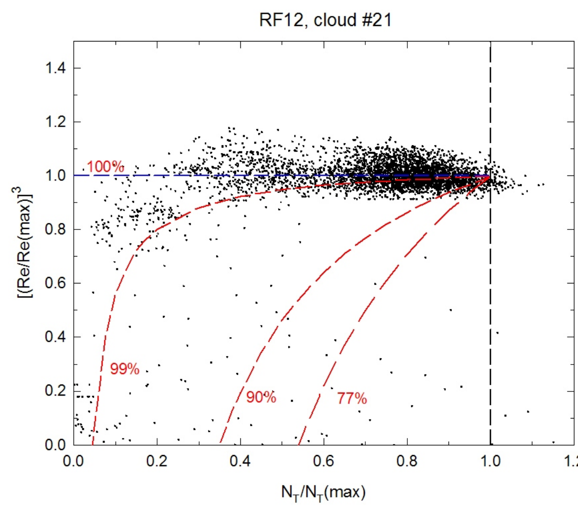

Fig. 4 - Normalized effective radius as a function of the total droplet concentration N_T for cloud #21. Percentages are RH values in the entrained air.

Here again the horizontal blue line represents extreme inhomogeneous mixing and the pattern of the data is similar to that of Fig. 3 and suggests that this mixing mechanism is taking place. The behavior of the data in both Figs. 3 and 4 show that Re is relatively constant while LWC (and ${}_t$) change substantially. This is in keeping with the earlier work by Blyth and Latham (1991) which also showed such stability of Re in Cu passes, and likewise suggested the dominance of extreme inhomogeneous mixing.

The red dashed lines in Fig. 4 indicate homogeneous mixing following entrainment where the different percentages represent the relative humidity (RH) of the ambient air that is entrained. The RH value of 77% is the ambient value measured some distance from the cloud, and the other RH values are hypothetical. The red lines can be calculated by using the conserved scalars of liquid water potential temperature and total water mixing ratio during the mixing process. This plot does not show the initial LWC dilution fractions which would form hyperbolas symmetrical with the x and y axes (see Burnet and Brenguier, 2006). The important feature of Fig. 4 is the tendency of increasing ambient RH to reduce the distinction between the extreme inhomogeneous and the homogeneous mixing; in fact at RH = 100% both mixing possibilities look the same. This possibility has been noted previously.

Many of the 35 Cu showed similar data behavior as shown in Figs. 3 and 4. But there were some that did not. Figures 5 and 6 show a cloud pass (cloud #6 at ~200 above LCL) with such different behavior. In figure 5 we see that many of the data points fall along the homogeneous-limit red line which indicates that LWC has changed in this

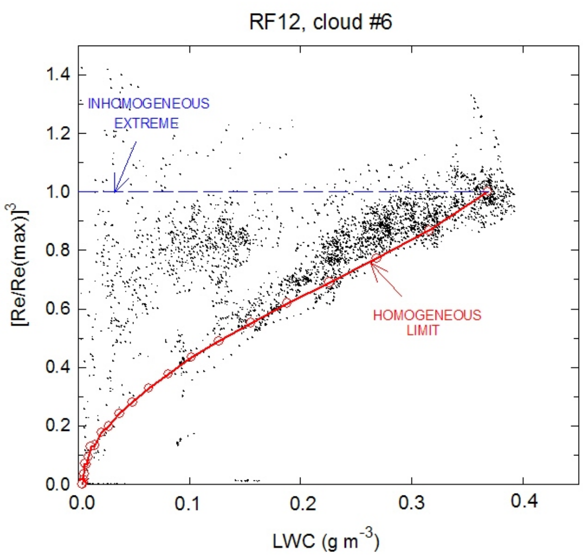

Fig. 5 - Normalized effective radius as a function of LWC in cloud pass #6.

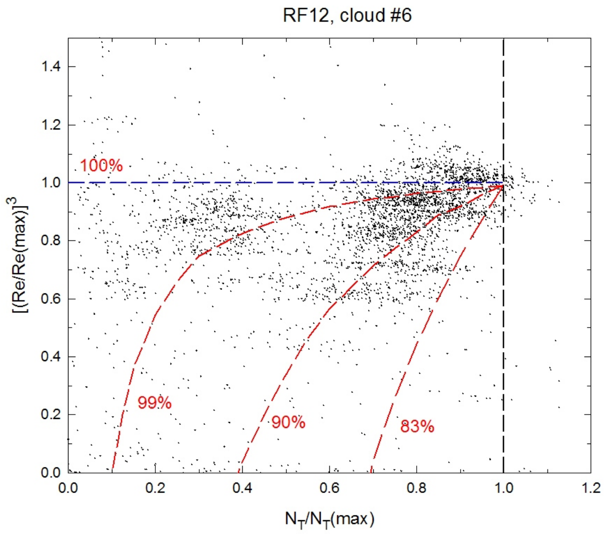

Fig. 6 - Normalized effective radius as a function of the total droplet concentration N_T. The percentages represent relative humidity in the entrained air.

Cu without any initial LWC dilution. Thus this pattern reflects cloud microphysical behavior that is not associated with the entrainment process affecting existing droplets. We interpret this data pattern as being either due to drops evaporating in descending cloud (which is unlikely in this case), or more likely being due to the activation and growth of new droplets formed on entrained CCN (cloud condensation nuclei). The corresponding plot of the same data in Fig. 6 now shows data scatter that can be incorrectly interpreted as entrainment followed by homogenous mixing with existing cloud droplets.

The different features of the data shown in Figs. 3 and 4 and Figs. 5 and 6 and used to establish either homogeneous or extreme inhomogeneous mixing appear throughout the 35 conditionally sampled Cu. Figure 7 gives a composite of the mixing behavior averaged for each of the 5 Cu levels. This figure was constructed by noting for all high-rate LWC data points their distance to the blue horizontal extreme inhomogeneous mixing line and by dividing this distance by the separation between the blue and the red homogeneous limit line as shown in Figs. 3 and 5. The resulting data is plotted in Fig. 7 as the extreme inhomogenous mixing fraction vs the height of the 5 flight levels above the LCL. We see

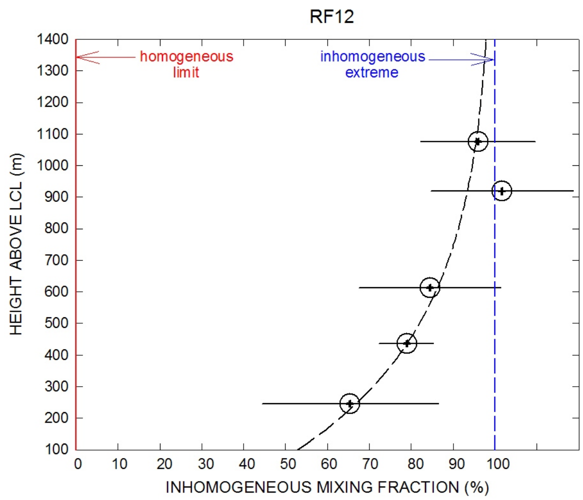

Fig. 7 - Average of the inhomogeneous mixing fraction for the Cu at the 5 levels flown by the C-130 aircraft. The horizontal lines are +/-1 sample standard deviation.

that there is a substantial gradient in this mixing fraction with height above the LCL, with the data apparently dominated by extreme inhomogeneous mixing as its proximity to the blue vertical dashed line shows. This tendency would be reduced if it were possible to take into account the initial LWC dilution in the Cu due to entrainment which is unknown given our inability to measure temperature and RH accurately and at high resolution in and near the Cu during RICO. As mentioned above, entrained air at high RH causing homogeneous mixing can not be differentiated from extreme inhomogenous mixing, so that the blue vertical dashed line could as well represent homogeneous mixing. Given that Cu detrain cloud that cools and humidifies the surrounding air makes this a reasonable possibility. It is tempting in this regard to extrapolate results described by Gerber et al (2005) for Sc that detrain and pre-condition air prior to entrainment to the trade-wind Cu. Regardless of whether humid homogenous mixing or extreme inhomogeneous mixing rules in the trade-wind Cu, the important result is that mixing followed by entrainment appears to be primarily a dilution effect, and deviations from this effect are caused primarily by the activation of new droplets on CCN introduced by entrainment into the Cu at all levels.

4. SCALE OF ENTRAINED PARCELS

Not much is known about the scale of the parcels of air that are entrained in Cu. Although, some modeling has suggested that these scales can be quite large (Brenguier and Grabowski, 1993; Krueger et al, 1997). Here we take advantage of the high rate LWC data to quantify the scale of these parcels in the 35 conditionally sampled trade-wind Sc. It had been noted earlier by Brenguier (1993) that the edges of Cu showed sharp gradients in droplet arrival times in his FFSSP droplet spectrometer. We note similar phenomena in the trade-wind Cu LWC data as the example in Fig. 8 shows. We assume in this data that rapid changes

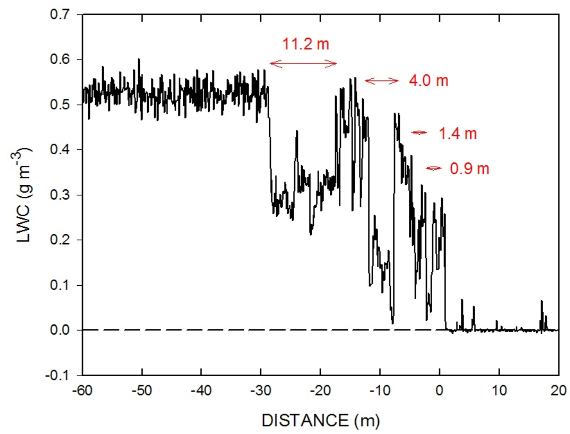

Fig. 8 - LWC as a function of distance from a Cu cloud edge. Red distances locate depleted LWC segments identified as entrained parcels.

in LWC over a small interval (3 data points which is equivalent to ~ 30 cm in cloud), and changes greater than the statistical sampling noise in the LWC data (as shown, for example, by the left portion of the LWC record in Fig. 8) indicate the presence of an entrained parcel. The lengths indicated in Fig. 8 show the distance over which the sharply depleted LWC exists, and this distance is defined as the entrained parcel length. This analysis was done for all conditionally sampled Cu in the lower four levels, the results of which are shown in Figs. 9 and 10. The highest level was not included, because these Cu were in the process of dissipating. We see that the entrained parcel length is relatively small with a mean value of about 2.4 m, has a log-normal probability distribution, and does not change significantly with height in the Cu. The log-normal behavior is significant, because if one assumes that the volume of air entrained is proportional to the entrainment length cubed, then this volume will also be log-normally distributed with the same geometric standard deviation but with a somewhat larger, but not excessive, volume median diameter.

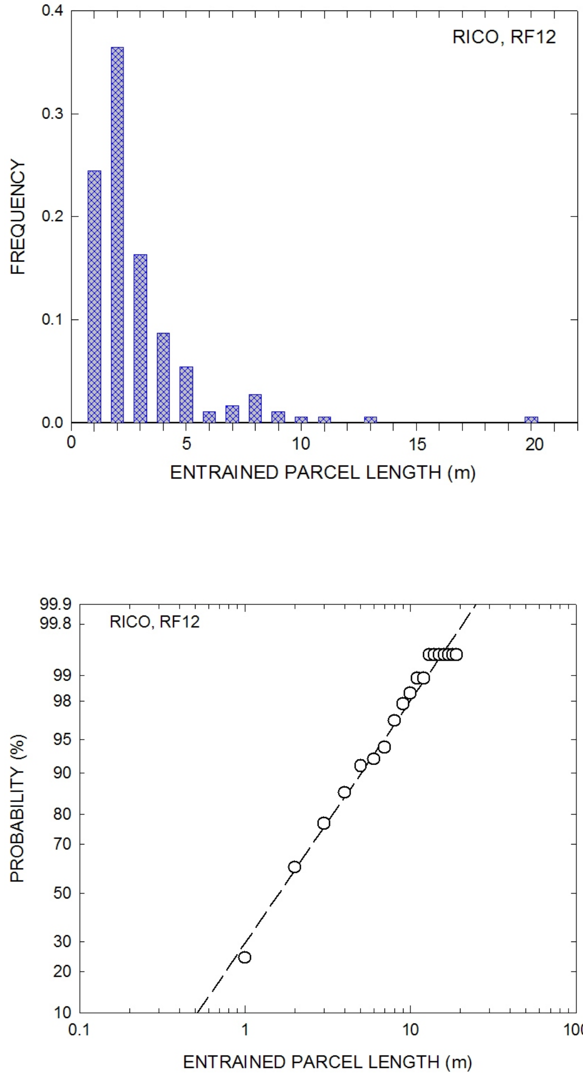

Figs. 9 and 10 - Composite of frequency (upper plot) and probability (lower plot) of entrained parcel length for all conditionally sampled Cu.

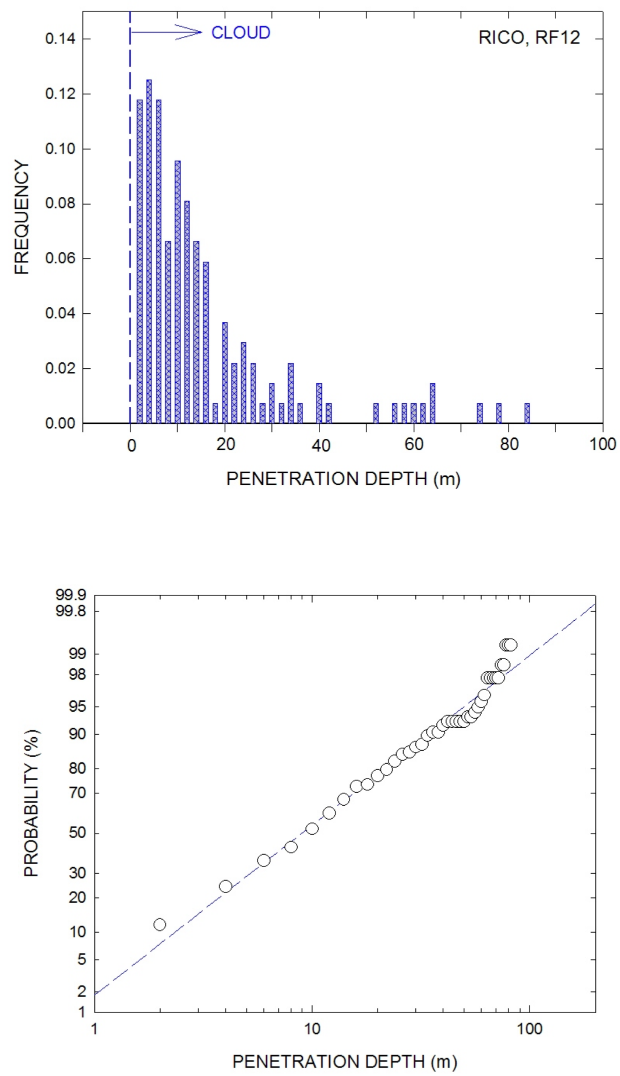

Figs. 11 and 12 - Composite of frequency (upper plot) and probability (lower plot) of entrained parcel penetration depth into the conditionally sampled Cu.

The search for the entrained parcels also provided their locations from the aircraft passes through the Cu in the lower 4 levels. The results are shown in Figs. 11 and 12 where their locations are seen to be primarily near cloud edge, and their distance from cloud edge is also log-normally distributed. The interior of these Cu were nearly devoid of entrained parcels as defined above. However, cloud segments with reduced LWC and with smoothed boundaries found in the interior suggests that these segments were originally entrained parcels at cloud edge but had already been modified by mixing with the existing cloud.

Given the relatively small size of the entrained parcels and the relatively large turbulent kinetic energy in the Cu indicates that the entrained parcels will have a short lifetime after introduction in the Cu. This finds support in that only ~3% of horizontal passes through the 35 Cu consists of cloud-free voids. These findings differ from the earlier estimates of larger entrainment scales. However, it must be borne in mind that here we are dealing with small active Cu turrets that may have their own unique characteristics in this regard.

5. RESPONSE TIME ANALYSIS

Cloud droplets have a response time $_{drop}$(s) given by ~ - $4r^2$/[4e-10 x (1-S)] for adjusting their sizes after being exposed to subsaturated entrained air, and entrained parcels have a response time $_{turb}$(s) given by ~ $(W^2/TKE_{diss})^{1/3}$ to fully mix with the existing cloud; where r(m) is the droplet radius, S is the saturation (S=1 at RH = 100%), W (m) is the entrained parcel width, and TKE_{diss} is the turbulent kinetic energy dissipation rate listed in Table 1 and shown in Fig. 13 for the 5 Cu levels The ratio R = $_{drop}$(s)/ $_{turb}$(s) has been used earlier (Baker et al, 1980; Baker et al, 1984; Jensen and Baker,1989: Burnet and Brenguier, 2006) to estimate which of the mixing scenarios following entrainment were in effect. For R >> 1 it was thought that homogenous mixing dominated, because time for turbulent mixing was less than the droplet response time; and for R<<1 it was thought that extreme inhomogeneous mixing dominated, because droplet response was faster than mixing.

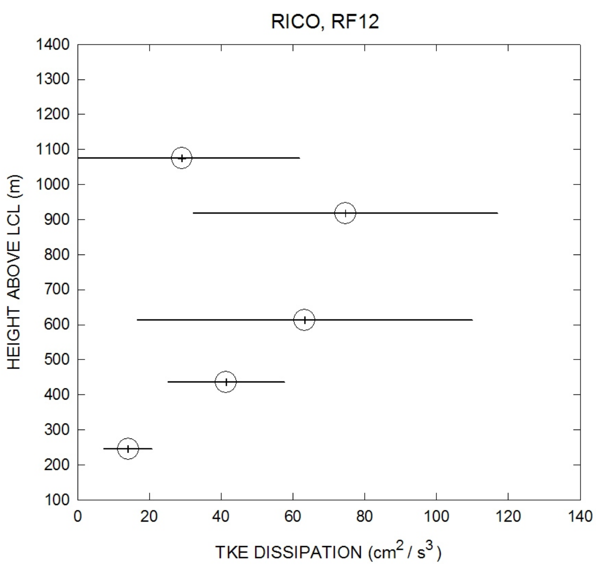

Fig. 13 - Average turbulent kinetic energy dissipation incloud for all conditionally sampled Cu at the 5 aircraft levels. Horizontal lines are +/- 1 sample standard deviation.

TABLE 2 - Response time ratio R for characteristic response times of turbulent mixing and droplet forcing (see text).

S	I	.77		:	.99	
$_{drop}$ (s)	I	5		:	100	
W (m)	I	2	20	:	2	20
$_{turb}$ (s)	I	8.5	40	:	8.5	40
R	I	.59	.12	:	12	2.5

Here the response time analysis is done for one trade-wind Cu (#21). Table 2 gives the result of calculating R given two initial values of RH in the entrained air with one being the “ambient” 77% value, a droplet radius of 10e-5 m, and two values for entrained parcel width W with one value being the ~2.5 m observed value (as pointed out by Jensen et al, 1985, the dissipation time constant of turbulent mixing with respect to droplet response should be the Kolmorgorov scale rather than W as noted by Baker et al, 1984; however, this difference just reinforces the point made here).The blue value (.12) of R in Table 2 reflects the smallest value shown and corresponds to rapid droplet response and the larger value of W, and thus corresponds to inhomogeneous mixing. The red value of R (12) is the largest shown and it reflects the strong effect of S being close to 100% RH, and the effect of the relatively small value of W, and thus corresponds to homogeneous mixing. Figure 13 shows a strong gradient with height in the Cu of the TKE dissipation. Given that the mixing time constant is proportional to the 1/3 power of the TKE dissipation does not change the results in Table 2 a great deal, but it suggests that near cloud base the value of R increases somewhat. We conclude that if the entrained air is cooled and moistened by conditioning with detrained cloud and since the entrained parcels are small, homogeneous mixing mechanism will dominate in these trade-wind Cu.

6. CONCLUSIONS

a. The average effect of entrainment and mixing in the 35 conditionally-sampled active-turret trade-wind Cu on flight RF12 is to primarily dilute the clouds without large droplet size changes as illustrated by comparing the cube of the effective radius to LWC and droplet concentration measured at 10-cm resolution by the PVM-100A probe. The dilution effect could be caused by extreme inhomogeneous mixing or more likely by homogeneous mixing of entrained air with high humidity. The effect has a significant vertical gradient with less of a dilution process towards cloud base where the fractional entrainment (Table 1) is the largest.

b. Deviation from the dilution affect appears to be mostly due to the activation of new droplets on CCN contained in the entrained air. This broadens the droplet spectra by generating new and smaller droplets at all levels and resulting in a nearly constant mean droplet concentration with height above cloud base.

c. Analysis of the turbulence mixing time scales (Table 1) and the droplet time response to sub-saturated forcing caused by entrainment (Table 2) suggests that homogeneous mixing with small-scale entrained air at high humidity is the principal mixing mechanism.

d. The fractional entrainment as a function of height above the LCL is large enough so that few droplets activated at cloud base reach cloud top. This vigorous entrainment rapidly reduces LWC below adiabatic values and reduces the mean volume radius much below the expected adiabatic values of this radius because of values of the vapor mixing ratio in the entrained air being smaller than this ratio incloud.

e. The average scale (~2.5 m) of the entrained parcels is smaller than expected and is lognormally distributed, as is their location near the edges of the Cu. A consequence of this relatively small entrained-parcel size is that the entrained parcels are rapidly mixed with the rest of the cloud and do not penetrate unchanged far into the Cu interior. This is supported by the observation that the interior of these Cu are virtually devoid of cloud-free volumes. A further consequence is that the compilations of the entrainment/mixing effects done here for the 5 Cu levels separated by ~200 m are in essence independent, because, given the measured incloud vertical velocities, the entrained parcels mix with the Cu before the Cu grow vertically another 200 m.

f. The rapid mixing of the small entrainment parcels also suggests that enhanced super-adiabatic droplet growth in strongly LWC depleted regions should not play a major role. Such regions were not found in the high rate Re data; however, this data is noisy making such a judgment difficult.

g. It is not known if the entire influence of entrainment is caused by the small-scale entrainment-parcel features found near Cu edges, because these Cu were conditionally sampled using aircraft penetrations ~ 200 m below cloud top thus preventing insights on behavior deeper in the Cu.

h. It is of interest to note that the results of the present study support the early conceptual ideas (e.g., Scorer and Ludlam, 1953) of erosion (detrainment) and entrainment in the bubble-wake type Cu model.

Finally, it must be kept in mind that the present attempt to establish observationally the average vertical behavior of the trade-wind Cu at 5 levels above cloud base on flight RF12 with respect to entrainment and the mixing mechanisms does not necessarily describe accurately the vertical evolution of these Cu. Individual aircraft passes through the Cu are not the desired vertical Lagrangian measurements incloud (which are impractical) needed to get accurate vertical evolution. For example, given our aircraft-pass approach we do not know if the Cu formed in volumes previously modified by earlier Cu, or if the Cu had a life history that does not resemble the vertical evolution of single active turrets.

ACKNOWLEDGEMENTS

Thanks are due Bjorn Stevens, Robert Rauber, Harry Ochs, and Charlie Knight for organizing RICO. Appreciation is expressed to the Research Aviation Facility of NCAR for their excellent running of RICO. This work was supported by NSF grant ATM-0345695.

REFERENCES

Baker, M.B., R.G. Corbin, and J. Latham, 1980: The influence of entrainment on the evolution of cloud droplet spectra. I. A model of inhomogeneous mixing. *Quart. J. Roy. Meteor. Soc.*, **106**, 581-598.

_________, R.E. Breidenthal, T.W. Choularton,, and J. Latham, 1984: The effects of turbulent mixing in clouds. *J. Atmos. Sci.*, **41**, 299-304.

Blyth, A.M., W.A. Cooper, and J.B. Jensen, 1988: A study of the source of entrained air in Montana cumuli. *J. Atmos. Sci.*, **45**, 3944-3964.

__________, and J. Latham, 1991: A climatological parameterization for cumulus clouds. *J. Atmos. Phys.*, **48**, 2367-2371.

Brenguier, J.-L., 1993: Observation of cloud microstructure at the centimeter scale. *J. Appl. Meteor.*, **32**, 783-793.

Burnet, F., and J.-L Brengier, 2006: Observational study of the entrainment-mixing process in warm convective clouds. *J. Atmos. Sci.*, in print.

Gerber, H., J.B. Jensen, A.B. Davis, A. Marshak, and. W. Wiscombe, 2001: Spectral density of cloud liquid water content at high frequencies. *J. Atmos. Sci.*, **58**, 497-503.

_________, G. Frick, S.P. Malinowski, J.-L. Brenguier, and F.Burnet, 2005: Holes and entrainment in stratocumulus. *J. Atmos. Sci.*, **62**, 443-459.

Jensen, J.B., and M.B. Baker, 1989: A simple model of droplet spectral evolution during turbulent mixing. *J. Atmos. Sci.*, **46**, 2812-2829.

Krueger, S.K, C.-W. Su, and P.A. McMurtry, 1977: Modeling entrainment and finescale mixing in cumulus clouds. *J. Atmos. Sci.*, **54**, 2697-2712.

Lasher-Trapp, S.G., W.A. Cooper, and A.M. Blyth, 2005: Broadening of droplet size distributions from entrainment and mixing in a cumulus cloud. *Quart. J. Roy. Meteor. Soc.*, **131**, 195-220.

Raga, G.B., J.B. Jensen, and M.B. Baker, 1990: Characteristics of cumulus band clouds off the coast of Hawaii. *J. Atmos. Sci.*, **47**, 338-355.

Schlueter, M.H., 2006: The effects of entrainment and mixing processes on the droplet size distributions in cumuli. Master Thesis. University of Utah, Salt Lake City, Utah.

Scorer, R.S., and F.H. Ludlam, 1953: Bubble theory of penetrative convection. *Quart. J. Roy. Meteor. Soc.*, **79**. 317-341.

Warner, J., 1955: The water content of cumuliform cloud. *Tellus*, **7**, 449-357.